Molecular Vision 2013; 19:2451-2467 <http://www.molvis.org/molvis/v19/2451>
Received 2 April 2013 | Accepted 26 November 2013 | Published 29 November 2013

Lenticular mitoprotection. Part B: GSK-3β and regulation of mitochondrial permeability transition for lens epithelial cells in atmospheric oxygen

Morgan M. Brooks, Sudha Neelam, Patrick R. Cammarata

Department of Cell Biology and Anatomy, University of North Texas Health Science Center at Fort Worth, Fort Worth, TX

Purpose: Loss of integrity of either the inner or outer mitochondrial membrane results in the dissipation of the mitochondrial electrochemical gradient that leads to mitochondrial membrane permeability transition (mMPT). This study emphasizes the role of glycogen synthase kinase 3beta (GSK-3β) in maintaining mitochondrial membrane potential, thus preventing mitochondrial depolarization (hereafter termed mitoprotection). Using 3-(2,4-dichlorophenyl)-4-(1-methyl-1H-indol-3-yl)-1H-pyrrole-2,5-dione (SB216763), an inhibitor of GSK-3β, and drawing a distinction between it and 1,4-diamino-2,3-dicyano-1,4-bis[2-aminophenylthio] butadiene (UO126), an inhibitor of extracellular-signal-regulated kinase (ERK) phosphorylation, the means by which GSK-3β influences mitoprotection in cultured human lens epithelial (HLE-B3) cells and normal, secondary cultures of bovine lens epithelial cells, maintained in atmospheric oxygen, was investigated.

Methods: Virally transfected human lens epithelial cells (HLE-B3) and normal cultures of bovine lens epithelial cells were exposed to acute hypoxic conditions (about 1% O_2) followed by exposure to atmospheric oxygen (about 21% O_2). Specific antisera and western blot analysis was used to examine the state of phosphorylation of ERK and GSK-3β, as well as the phosphorylation of a downstream substrate of GSK-3β, glycogen synthase (GS, useful in monitoring GSK-3β activity). The potentiometric dye, 1H-benzimidazolium-5,6-dichloro-2-[3-(5,6-dichloro-1,3-diethyl-1,3-dihydro-2H-benzimidazol-2-ylidene)-1-propenyl]-1,3-diethyl-iodide (JC-1), was used to monitor mitochondrial depolarization upon exposure of inhibitor treatment relative to the control cells (mock inhibition) in atmospheric oxygen. Caspase-3 activation was scrutinized to determine whether mitochondrial depolarization inevitably leads to apoptosis.

Results: Treatment of HLE-B3 cells with SB216763 (12 μM) inactivated GSK-3β activity as verified by the enzyme's inability to phosphorylate its substrate, GS. SB216763-treated cells were not depolarized relative to the control cells as demonstrated with JC-1 fluorescent dye analysis. The HLE-B3 cells treated with UO126, which similarly blocked phosphorylation of GS, were nevertheless prone to mMPT relative to the control cells. Western blot analysis determined that Bcl-2-associated X (BAX) levels were unchanged for SB216763-treated or UO126-treated HLE-B3 cells when compared to their respective control cells. However, unlike the SB216763-treated cells, the UO126-treated cells showed a marked absence of Bcl-2, as well as phosphorylated Bcl-2 relative to the controls. UO126 treatment of bovine lens epithelial cells showed similar results with pBcl-2 levels, while the Bcl-2 content appeared unchanged relative to the control cells. HLE-B3 and normal bovine lens cell cultures showed susceptibility to mMPT associated with the loss of pBcl-2 by UO126 treatment.

Conclusions: Mitochondrial depolarization may occur by one of two key occurrences: interruption of the electrochemical gradient across the inner mitochondrial membrane resulting in mMPT or by disruption of the integrity of the inner or outer mitochondrial membrane. The latter scenario is generally tightly regulated by members of the Bcl-2 family of proteins. Inhibition of GSK-3β activity by SB216763 blocks mMPT by preventing the opening of the mitochondrial permeability transition pore. UO126, likewise, inhibits GSK-3β activity, but unlike SB216763, inhibition of ERK phosphorylation induces the loss of intracellular pBcl-2 levels under conditions where intracellular BAX levels remain constant. These results suggest that the lenticular mitoprotection normally afforded by the inactivation of GSK-3β activity may, however, be bypassed by a loss of pBcl-2, an anti-apoptotic member of the Bcl-2 family. Bcl-2 prevents the translocation of BAX to the mitochondrial outer membrane inhibiting depolarization by disrupting the normal electrochemical gradient leading to mMPT.

The dissipation of mitochondrial membrane potential ($\Delta\Psi$) occurs in a process termed mitochondrial permeability transition (mMPT) [1]. Lens epithelial cells represent an ideal model for studying mMPT because the lens thrives in a naturally hypoxic environment, and introducing atmospheric oxygen increases the formation of reactive oxygenated species (ROS), which, in turn, may cause a loss of $\Delta\Psi$ [1,2]. The current literature suggests that mMPT is mediated

Correspondence to: Dr. Patrick R. Cammarata, Department of Cell Biology and Anatomy, University of North Texas Health Science Center at Fort Worth, 3500 Camp Bowie Boulevard, Fort Worth, TX, 76107; Phone: (817) 735-2045; FAX: (817) 735-2610; email: patrick.cammarata@unthsc.edu

via the opening of the mitochondrial permeability transition pore [3-5]. Studies have shown that glycogen synthase kinase 3beta (GSK-3β) is immediately proximal to the mitochondrial permeability transition pore and acts as a point of integration for many protective signals [6]. Thus, GSK-3β is a crucial enzyme involved in preventing mMPT through regulating the opening and closing of the mitochondrial permeability transition pore [7,8]. Additional studies involving ischemic reperfusion of cardiac myocytes have demonstrated that inhibiting GSK-3β can prevent the dissipation of ΔΨ during oxidative stress [9-11].

One of the multiple protective proteins that converge on GSK-3β is the phosphorylated form of extracellular signal-regulated kinase (ERK) [12]. Flynn et al. [1] has previously demonstrated that after RNA suppresses ERK ΔΨ collapses during oxidative stress in human lens epithelial cells (HLE-B3) cells. Furthermore, studies conducted on metastatic carcinoma cells have shown that phosphorylated ERK can cause GSK-3β to become phosphorylated at its inhibitory serine, thus inactivating the enzyme [12]. Combined, these studies suggest that ERK can prevent the disruption of ΔΨ by inactivating GSK-3β, presumably blocking the opening of the mitochondrial transition pore. However, as will be demonstrated in this study, inhibiting ERK phosphorylation can, itself, cause mitochondrial depolarization regardless of the activity of GSK-3β.

To date, the role that GSK-3β plays regarding preventing mitochondrial depolarization has not been established in an ocular system. In the current study, we demonstrate that inactivating GSK-3β activity (as monitored by its failure to phosphorylate glycogen synthase) using the pharmacological inhibitor SB216763 has a regulatory function in preventing mitochondrial depolarization. Furthermore, this study will reveal that the mitoprotection normally afforded by GSK-3β inactivation may be circumvented by inhibiting ERK phosphorylation, which culminates in inhibition of Bcl-2 phosphorylation, an anti-apoptotic member of the Bcl-2 family.

METHODS

Materials: The Mitogen Activated Protein Kinase-1/2 (MEK1/2) inhibitor 1,4-diamino-2,3-dicyano-1,4-bis[2-aminophenylthio] butadiene (UO126) was purchased from Cell Signaling Technology (Danvers, MA). The glycogen synthase kinase inhibitor 3-(2,4-dichlorophenyl)-4-(1-methyl-1H-indol-3-yl)-1H-pyrrole-2,5-dione (SB216763) was purchased from Sigma-Aldrich (St. Louis, MO). The c-Jun N-terminal kinase (JNK) inhibitors SP600125 (JNK Inhibitor II) and AS601245 (JNK Inhibitor V) were purchased from EMD Millipore Chemicals (Billerica, MA). Stock inhibitors were prepared by adding to dimethyl sulfoxide (DMSO) as follows: 20 mM for UO126, 16 mM for SB216763, 40 mM for SP600125, and 40 mM for AS601245. The mitochondrial dye 1H-benzimidazolium-5,6-dichloro-2-[3-(5,6-dichloro-1,3-diethyl-1,3-dihydro-2H-benzimidazol-2-ylidene)-1-propenyl]-1,3-diethyl-iodide (JC-1) was obtained from Life Technologies (Grand Island, NY). All other reagents were acquired from other commercially available sources as previously reported [1].

Cell cultures: HLE-B3 cells, a human lens epithelial cell line immortalized by the SV-40 virus [13], were obtained from U. Andley (Washington University School of Medicine, Department of Ophthalmology, St. Louis, MO). Authentication of the HLE-B3 cell line was verified with STR profile analysis (American Type Culture Collection, Manassas, VA), which confirmed that the cell line was human and of female origin, as originally reported by Andley et al. [13]. A copy of the STR profile is available upon request. All studies with HLE-B3 cells were performed with prefrozen stock cells (maintained in liquid nitrogen) between passages 14 and 17. No experiments exceeded five passages beyond the initial stock cell passage. The cells were maintained in minimal essential media (MEM) containing 5.5 mM glucose supplemented with 20% fetal bovine serum (Gemini Bio-Products, Sacramento, CA), 2 mM L-glutamine, nonessential amino acids, and 0.02 g/l gentamycin solution (Sigma-Aldrich) and cultured at 37 °C and 5% CO_2–95% O_2 [1]. Cells were sub-cultured 4 to 5 days before the experiment and placed in MEM containing 20% fetal bovine serum (FBS). Twenty-four hours before the day of the experiment, the cells were switched to serum-free MEM. Unless otherwise specified, all experiments followed a common protocol: Cells were maintained in atmospheric O_2 (about 21%) for 90 min, then switched to hypoxic conditions (about 1% O_2) for 180 min, followed by reintroduction to atmospheric O_2. Each experiment was executed with control DMSO-only cells (mock inhibitor treatment) and cells treated with inhibitors. The DMSO concentration per experiment never exceeded 0.05%.

Bovine eyes obtained from a local abattoir were transported on ice to the laboratory, where the lenses were removed aseptically. Bovine lens epithelial cells (BLECs) were isolated and cultured in 20% bovine calf serum–supplemented Eagle's minimal essential medium. All studies with BLECs were performed on cells of passage 2.

Western blot analysis: Whole cell lysates were collected from HLE-B3 cultures using the hot protein extraction method as described by Henrich et al. [14]. The cell cultures were rinsed at room temperature in final concentration: 150 mM sodium chloride, 10 mM sodium phosphate monobasic, 40 mM

sodium phosphate dibasic), pH 7.4, before the monolayers were lysed with hot lysis buffer (about 100 °C), subsequently scraped into 1.7 ml micro centrifuge tubes, and immediately sonicated. The lysis buffer consisted of 0.12 M Tris-HCl (pH 6.8), 4% sodium dodecyl sulfate (SDS), and 20% glycerol [1]. Part of the lysate samples were removed and used to determine the protein concentration. The protein concentration was calculated by using a DC protein assay kit from Bio-Rad (Hercules, CA). The lysate samples contained 25 µg of protein, 1X SDS laemmli buffer, and 1.5 µl 2-mercaptoethanol (Sigma-Aldrich). The lysate samples were then boiled for 5 min and the proteins resolved on 12% SDS-polyacrylamide gels. The proteins were then transferred to a nitrocellulose membrane (Bio-Rad). The electrophoresis and western blot apparatus were from Hoefer Scientific (Holliston, MA).

For western blot analysis, nitrocellulose membranes were blocked with 0.1% BSA and 0.02% Tween-20 in Tris-buffered saline (TTBS) for 60 min. These membranes were probed overnight at 4 °C with primary antibodies at a 1:1,000 dilution. The blots were then rinsed in TTBS for 5 min 4X and then incubated in either goat anti-rabbit horseradish peroxidase conjugate or goat anti-mouse horseradish peroxidase conjugate at 1:10,000 dilution (Santa Cruz Biotechnology, Santa Cruz, CA) for 60 min at room temperature. Blots were again rinsed in TTBS (4X 5 min washes), and proteins were detected using a SuperSignal West Pico chemiluminescent kit from Pierce (Rockford, IL) [1]. Probed membranes were visualized on a Fluoro Chem TM 8900 imager (Alpha Innotech, San Leandro, CA).

Primary antibodies were purchased from Cell Signaling Technology (Danvers, MA). The antibodies used in this study included rabbit anti-Bcl-2-associated X (BAX), rabbit anti-glycogen synthase, rabbit anti-phosphoglycogen synthase (Ser641), rabbit anti-phospho-GSK-3β (Ser9), rabbit anti-GSK-3β, mouse anti-phospho-p44/42 mitogen-activated protein kinase (Thr202/Tyr204), rabbit anti-p44/42 mitogen-activated protein kinase, rabbit anti-phospho-Bcl-2 (Ser70), rabbit anti-Bcl-2, and rabbit anti-phospho-c-Jun (Ser63). Rabbit anti-actin was provided by Santa Cruz Biotechnology (Santa Cruz, CA).

JC-1 fluorescence analysis and confocal microscopy: After the HLE-B3 cells were subjected to inhibitor treatments, the cells were stained with JC-1 to determine the mitochondrial membrane potential. JC-1 is a membrane permeant lipophilic dye that exists as J-aggregates in the mitochondrial matrix (red fluorescence) and as monomers in the cytoplasm (green fluorescence). During mitochondrial depolarization, the red J-aggregates flow out of the mitochondria and accumulate in the cytosol as green monomers [15]. Thus, depolarization can be measured as an increasing green fluorescent/red fluorescent intensity ratio.

The JC-1 assay was performed as follows. HLE-B3 cell monolayers were maintained in serum-free MEM with or without inhibitor treatment, brought through atmospheric oxygen into hypoxia, and then later switched back to atmospheric oxygen as described above. At the end of the hypoxic exposure, the hypoxic media on cells (oxygen depleted) were poured off, and fresh (oxygen rich) serum-free MEM (with or without an inhibitor) was added containing 5 µg/ml JC-1 for 30 min in a tissue culture incubator. The stained HLE-B3 cells were then rinsed twice using serum-free MEM, and fresh oxygenated serum-free MEM (with or without inhibitor, but no JC-1 dye) was added. A random field of cells was imaged every 2.5 min for 60 min using an X10 objective on a confocal microscope (Ziess LSM410, LSM410, Thornwood, NY). The excitation wavelength was 488 nm, and the microscope was set to simultaneously detect green emission (540 nm) and red emission (595 nm) channels using a dual bandpass filter [1].

Caspase-3 apoptosis detection assay: A caspase-3 enzyme-linked immunosorbent assay (ELISA; Invitrogen, Camarillo, CA) was used to determine apoptosis. HLE-B3 cell monolayers were maintained in serum-free MEM with or without treatment and brought through our experimental protocol, which included atmospheric oxygen into 3 h of hypoxia, and then subsequently switched back to atmospheric oxygen. Treatment included SB216763 (12 µM), UO126 (10 µM), staurosporine (100 nM), or 0.05% DMSO vehicle maintained throughout the course of the experiment. Sixty minutes after atmospheric oxygen was reintroduced, all samples were then lysed using our lysis buffer (0.12 M Tris-HCl [pH 6.8], 4% SDS, and 20% glycerol). Part of the lysate samples was removed and used to determine the protein concentration. The protein concentration was calculated by using a DC protein assay kit (Bio-Rad). Apoptotic activity was determined following the manufacturer's protocol using 10 µg of protein.

Statistical analysis: Images from JC-1 confocal microscopy were separated into individual red and green channels using ImageJ (Baltimore, MD). The background fluorescence was removed from each image before the intensity was measured. The fluorescence intensity signal from each image was quantified for the entire image and expressed as the ratio of green fluorescent intensity over red fluorescent intensity. Western blot densitometry was determined using ImageJ, and related statistics was determined using GraphPad Prism 5 (La Jolla, CA).

RESULTS

Switching HLE-B3 cell cultures from hypoxia to atmospheric oxygen or, conversely, from atmospheric oxygen to hypoxia, does not induce mitochondrial depolarization: JC-1 analysis of the DMSO mock-treated cells exposed to various cell culture conditions was implemented to determine whether environmental stress (i.e., hypoxia, atmospheric oxygen, or reversal from one condition to the other) elicited mitochondrial depolarization. Four conditions were tested: cells grown in constant atmospheric oxygen, cells switched from atmospheric oxygen to hypoxia, cells switched from hypoxia to atmospheric oxygen, and cells maintained in continuous hypoxia. Under all tested conditions, the cells did not depolarize, indicating that continuous hypoxia, atmospheric oxygen, and switching cell culture environments (hypoxia to atmospheric oxygen or atmospheric oxygen to hypoxia) do not induce depolarization (Figure 1).

SB216763 inhibits the enzymatic activity of GSK-3β and prevents mitochondrial depolarization during oxidative stress: To investigate the role GSK-3β plays in regulating cellular mitoprotection with cells maintained in hypoxia and subsequently exposed to atmospheric oxygen, HLE-B3 cells were treated with the GSK-3β inhibitor, SB216763. Non-phosphorylated GSK-3β is the active form of the enzyme, and in this form, the enzyme is capable of phosphorylating numerous downstream substrates including glycogen synthase (GS) [16]. The phosphorylation of GS is thus a useful parameter for monitoring GSK-3β activity. Cultures of HLE-B3 cells were grown on 100 mm dishes until >85% confluence. Cells were treated with 12 µM SB216763 or mock-treated with DMSO (control). After 90 min in ambient oxygen, the cells were placed under hypoxic conditions (about 1% O_2) for 3 h and then switched back to atmospheric oxygen (about 21% O_2) for 3 h. Samples were collected from cells consistently maintained in atmospheric oxygen (control), immediately after hypoxic exposure and 1 h, 2 h, and 3 h of reexposure to atmospheric oxygen. Western blot analysis showed that the HLE-B3 cells subjected to SB216763 treatment had levels of GSK-3β and phosphoglycogen synthase kinase-3beta (pGSK-3β) similar to those of the controls (Figure 2). However, treatment with SB216763 resulted in inhibition of phosphorylation of GS. The failure to phosphorylate GS indicates the active site of GSK-3β was inactivated. The continued presence of pGSK-3β in the treated cells was because the autophosphorylation site of GSK-β was unaffected by SB216763 [17]. A key question that we wished to address in this study was whether inhibiting GSK-3β activity positively correlated with preventing mitochondrial depolarization. In a recent related study [18], we observed that SB216763-treated cells monitored for mMPT using emission spectroscopy displayed suppressed mitochondrial depolarization relative to the control DMSO mock-treated cells.

ERK1/2 inhibition prompts depolarization without affecting pGSK-3β under oxidative stress conditions: A parallel experiment, using the MEK1/2 inhibitor, UO126, was also conducted on HLE-B3 cells to determine whether inhibiting ERK1/2 phosphorylation had any impact on the phosphorylation of GSK-3β and GS. Lens cells were treated with 10 µM UO126 or DMSO and subsequently placed in hypoxic conditions for 3 h. Following the hypoxic exposure, new media were added to the culture dishes, and the cells were exposed to atmospheric oxygen for up to 3 h in the continued presence and absence of UO126. Lysates of these cells were collected from cells maintained consistently in atmospheric oxygen, after the hypoxic exposure and 1 h, 2 h, and 3 h after atmospheric oxygen was reintroduced. Analysis of the western blot membranes showed marked inhibition of p42 ERK1/2 and p44 ERK1/2 (Figure 3, upper panel, left) relative to the control cells. The loss of ERK1/2 phosphorylation did not affect the relative levels of GSK-3β or pGSK-3β compared with the DMSO controls (Figure 3, upper panel, right), whereas inhibiting ERK phosphorylation prevented the downstream phosphorylation of GS. Therefore, the configuration of the ratio of pGSK-3β/GSK-3β and pGS/GS appeared identical irrespective of whether SB216763 or UO126 was used (compare the bar graphs of Figure 2 and Figure 3). Given the similarity in the profile of the ratio of pGSK-3β/GSK-3β and pGS/GS, a critical question was whether UO126-treated cells, similar to SB216763-treated cells, likewise prevented mitochondrial depolarization relative to the control DMSO mock-treated cells or whether UO126-treated cells were prone to mMPT.

Parallel studies were conducted using JC-1 analysis. HLE-B3 cells were treated with 10 µM UO126 or DMSO and then placed under hypoxic conditions for 3 h. The cells were exposed to the JC-1 dye for 30 min in atmospheric oxygen. Following the JC-1 application, fresh media with U0126 or DMSO were added to the culture plates. The cells were subsequently observed with confocal microscopy and the green and red intensities recorded every 2.5 min for 60 min. The green to red ratio of the UO126-treated cells markedly increased over the time course relative to the control cells, indicating the loss of $\Delta\Psi$ (Figure 3, bottom panel).

SB216763 versus UO126 treatment on BAX, Bcl-2, and Bcl-2 phosphorylation levels: As discussed above, comparison of the western blots for pGSK-3β/GSK-3β and pGS/GS between the two inhibitor treatments generated profiles that were similar, if not, identical (compare Figure 2 and

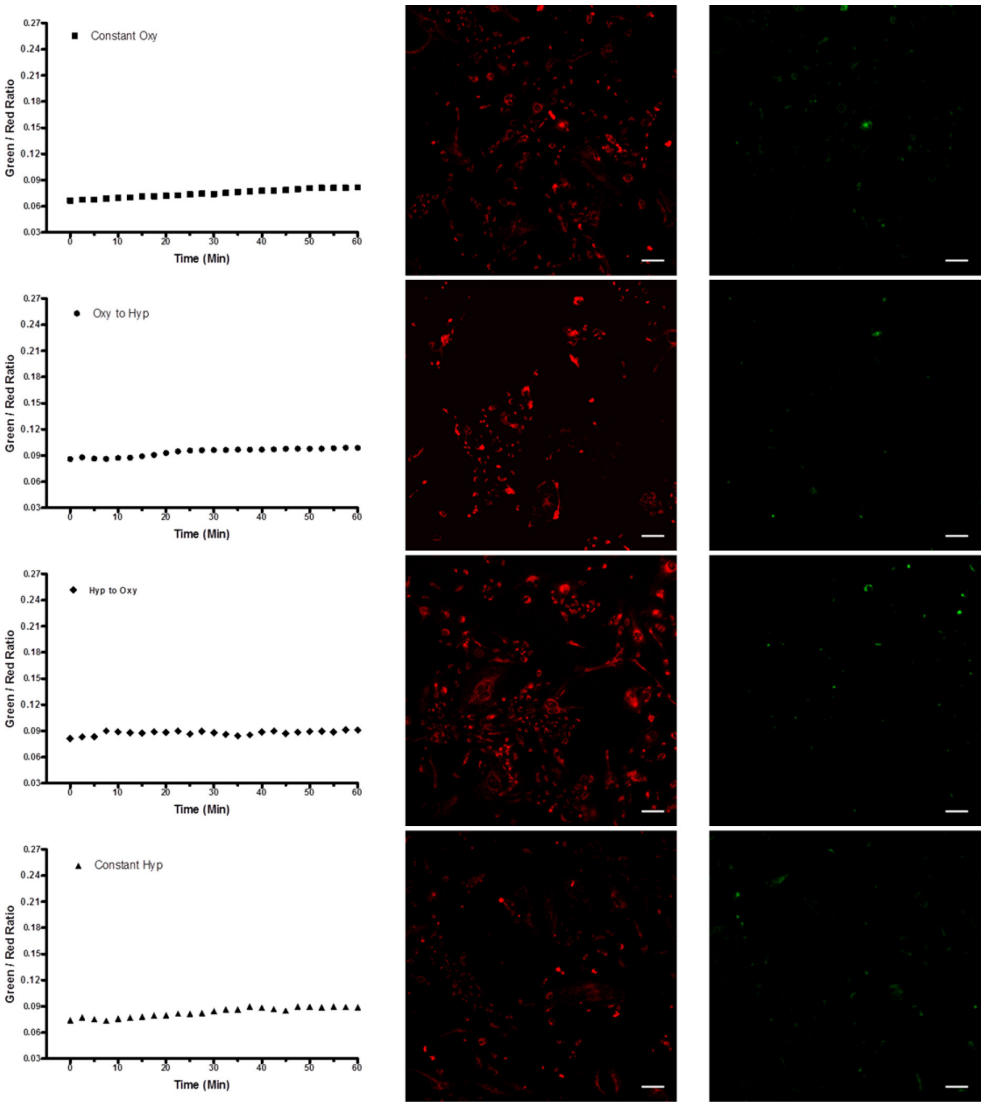

Figure 1. JC-1 stained mock treated (DMSO) HLE-B3 cells under several adaptations of hypoxic and atmospheric oxygen exposure. Human lens epithelial (HLE-B3) cells were stained with JC-1 (5 µg/ml) and observed with confocal microscopy with images captured every 2.5 min over a 60 min period, under the following conditions: (1) continuous hypoxia, (2) continuous atmospheric oxygen, (3) switching from hypoxia to atmospheric oxygen, or (4) switching from atmospheric oxygen to hypoxia. Top row: (continuous oxygen) HLE-B3 cells were maintained in atmospheric oxygen and stained for 30 min in atmospheric oxygen. At the end of the 30 min staining period, fresh oxygenated media without the JC-1 dye were added to the dishes. A random field of cells was then imaged. Note to the reader: The term "random field of cells" here and with all successive JC-1 analyses is meant to infer an arbitrary field of cells is selected, but once chosen, the same field of cells is photographed throughout the 60 min image capture. Second row: (atmospheric oxygen to hypoxia) HLE-B3 cells were maintained in atmospheric oxygen and stained for 30 min in atmospheric oxygen. At the end of the 30 min staining period, the cells were switched to hypoxic media (i.e., medium that had been preincubated at 1% oxygen). A random field of cells was immediately imaged. Third row: (hypoxia to atmospheric oxygen) HLE-B3 cells were placed in hypoxic conditions for 180 min. At the end of the hypoxic exposure, the media were removed and replaced with fresh oxygenated media containing JC-1. The cells were stained for 30 min in atmospheric oxygen. After this 30 min period, the media were again removed, and fresh oxygenated media were added without the JC-1 dye. A random field of cells was then imaged. Fourth row: (continuous hypoxia) HLE-B3 cells were stained with serum-free minimal essential media (MEM) cotaining JC-1 for 30 min in atmospheric oxygen. At the end of this 30 min period, the media were removed, and fresh medium that had been preincubated at 1% oxygen was added without the JC-1 dye. The cells were then switched into the hypoxic conditions for 180 min. The cells were imaged following the 3 h hypoxic exposure. Under all experimental conditions, there was no evidence of loss of membrane potential throughout the 60 min image capture.

Figure 3). However, whereas treatment with the GSK-3β inhibitor, SB216763, likely blocked opening of the mitochondrial membrane permeability transition pores, effectively suppressing depolarization [18], treatment with UO126 elicited profound depolarization relative to the control cells (Figure 3, bottom panel). We therefore examined in greater detail the outcome of each inhibitor on the BAX, Bcl-2, and pBcl-2 levels.

Lysates from all experimental treatments were evaluated to determine the levels of Bcl-2, pBcl-2, and BAX. Western blot membranes from the SB216763- and UO126-treated cells relative to their respective controls indicated no alteration in the levels of BAX for the treated and control cells (Figure 4,

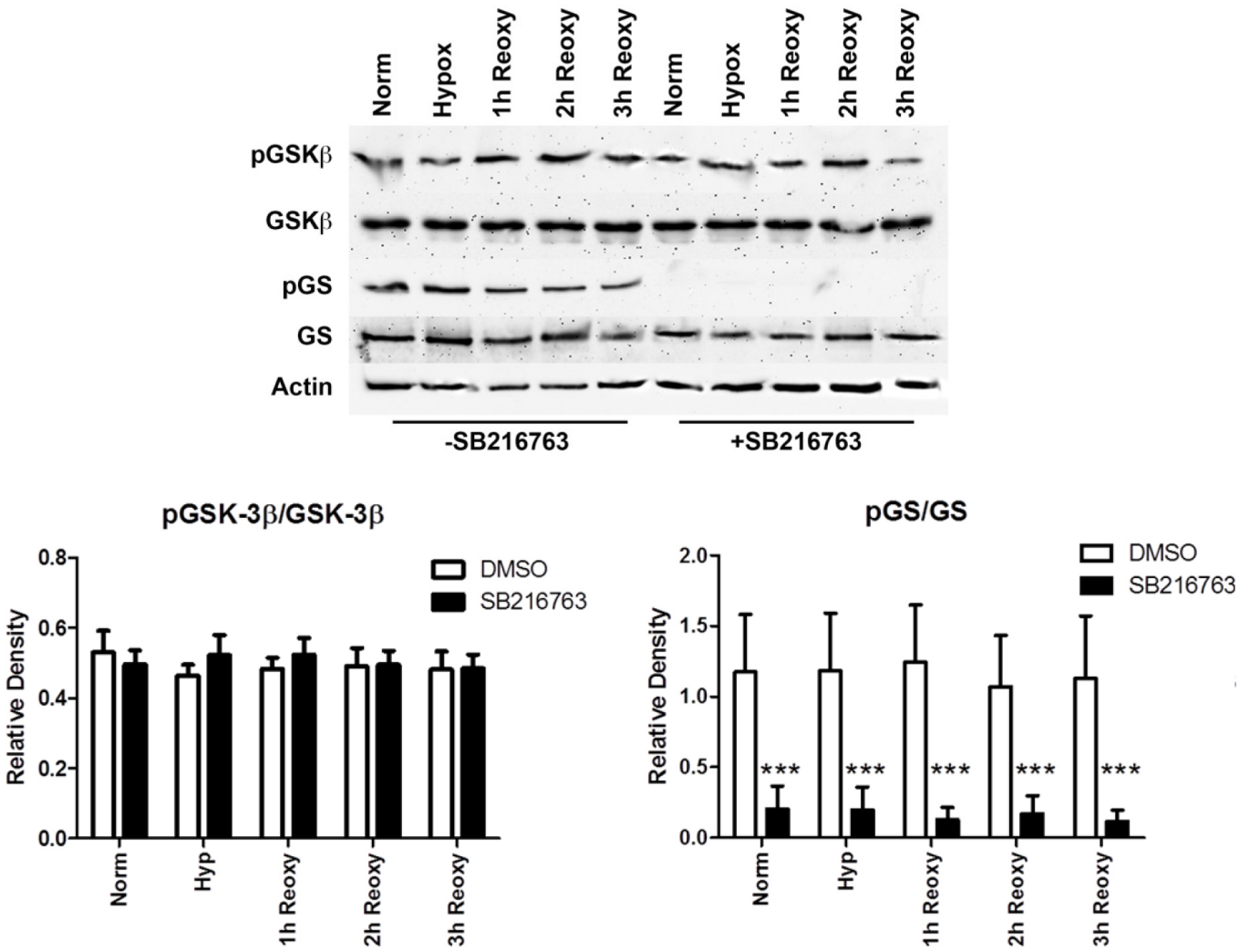

Figure 2. Western blot analysis of glycogen synthase kinase 3β and glycogen synthase phosphorylation in HLE-B3 cells in the presence or absence of SB216763. Total cell lysates were collected from >85% confluent human lens epithelial (HLE-B3) cell cultures that were incubated for 90 min in serum-free minimal essential media (MEM), under conditions of atmospheric oxygen, containing either 12 µM SB216763 or 0.05% DMSO vehicle. Cells were then exposed to hypoxia for 3 h in the continued presence of SB216763. At the end of the hypoxic incubation period, the hypoxic media were removed, and fresh, oxygenated serum-free MEM with SB216763 or DMSO vehicle were added to the cultures. Cells were then placed in atmospheric oxygen for up to 3 h. Cultures were collected after (1) continuous normoxic exposure (about 21% oxygen), (2) after the 3 h hypoxic exposure (about 1% oxygen), or (3) after reintroduction of atmospheric oxygen (about 21%) for 1, 2, or 3 h subsequent to the 3 h hypoxic exposure. Total cell lysates were analyzed with immunoblots using 25 µg of protein per lane. Anti-actin was used to normalize the bands to ensure equivalent lane loading. Three experiments, using independent cell populations, were quantified using GraphPad Prism 5 and the relative densities plotted for pGSK-3β/GSK-3β and pGS/GS. No change was evident in the ratio of pGSK-3β/GSK-3β while significant inhibition of the phosphorylation of glycogen synthase by SB216763 was noted. Error bars represent standard error. The asterisks (***) indicate $p<0.001$, Student *t* test.

upper panel and Figure 5, upper panel). The relative levels of pBcl-2 and Bcl-2 were not altered for the SB216763-treated cells compared with the control cells (Figure 4, middle panel). In contrast, the UO126-treated cells displayed significantly diminished levels of pBcl-2 under all culture conditions, including normoxic control, hypoxic exposure, and the reintroduction of oxygen subsequent to hypoxic exposure (Figure 5, middle panel); a significant loss of Bcl-2 was also observed but, interestingly, only during the reintroduction of oxygen phase (Figure 5, middle panel).

Of particular note, treatment with UO126 (Figure 5, upper panel, left and bottom panels) but not with SB216763 (Figure 4, upper panel left and bottom panel) prevented the phosphorylation of c-JUN, through all culture conditions.

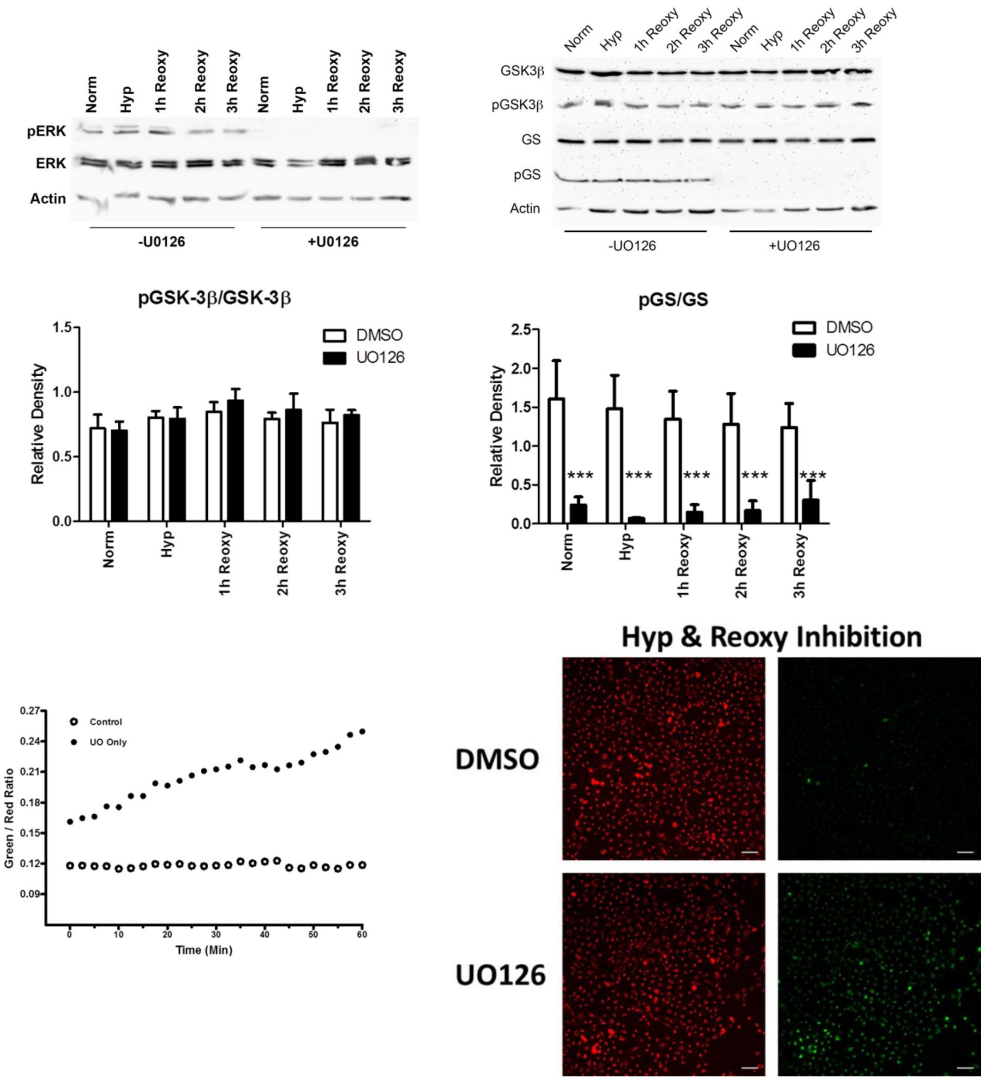

Figure 3. Western blot analysis of GSK-3β and GS phosphorylation in HLE-B3 cells treated with UO126 inhibitor. HLE-B3 cell cultures were incubated for 90 min in serum-free minimal essential media (MEM), under conditions of atmospheric oxygen, containing either 10 µM UO126 or 0.05% DMSO vehicle. Cells were then exposed to hypoxia for 3 h. At the end of the hypoxic incubation period, the hypoxic media were removed, and fresh, oxygenated serum-free MEM with UO126 or DMSO vehicle were added to the cultures. Cells were then placed in atmospheric oxygen for up to 3 h. Cultures were collected after (1) continuous normoxic exposure (about 21% oxygen), (2) after the 3 h hypoxic exposure (about 1% oxygen), or (3) after reintroduction of atmospheric oxygen (about 21%) for 1, 2, or 3 h subsequent to the 3 h hypoxic exposure. Total cell lysates were analyzed with immunoblots using 25 µg of protein per lane. Anti actin was used to normalize the bands to ensure equivalent lane loading. The loss of phosphorylation of ERK by UO126 treatment was noted (top, left panel), as was the loss of phosphorylated glycogen synthase by western blot analysis (top, right panel). Three experiments, using independent cell populations, were quantified using GraphPad Prism 5, and the relative densities were plotted for pGSK-3β/GSK-3β and pGS/GS. No change was evident in the ratio of pGSK-3β/GSK-3β while significant inhibition of the phosphorylation of glycogen synthase by UO126 was indicated (middle panel). Error bars represent standard error. The asterisks (***) indicate p<0.001, Student *t* test. (bottom panel, left) HLE-B3 cells were incubated for 90 min with serum-free MEM, under atmospheric condition, containing 10 µM UO126 or 0.05% DMSO vehicle. Cells were switched to hypoxia for 3 h in the continued presence of UO126 or DMSO vehicle. At the end of the hypoxic exposure, the cells had their media removed, and fresh, oxygenated serum-free MEM containing 5 µg/ml JC-1 and either UO126 or DMSO added for 30 min in atmospheric oxygen. At the end of the 30 min incubation period, the media were again switched with fresh serum-free MEM containing UO126 or DMSO in the absence of the JC-1 dye. The same field of cells was imaged every 150 s for 60 min. Serial confocal imaging of mitochondrial depolarization in HLE-B3 cells in the presence of UO126 demonstrated significant depolarization compared to control cells. (bottom panel, left) Images of the red and green intensity for the UO126- and DMSO-treated cells at t=60 min (bar=20 µm). Note the marked intensity of the green channel with UO126-treated cells relative to DMSO mock treatment at the completion of the 60 min analysis (bottom panel, right) indicating mitochondrial depolarization.

The phosphorylation of c-Jun is a useful parameter for monitoring JNK activity. That is, UO126, while effectively inhibiting ERK phosphorylation (refer to Figure 3, upper panel, left), was nonetheless equally effective in inactivating JNK activity. This observation imposed a burden of proof upon us to determine whether the ERK pathway or the JNK pathway negatively impacted the pBcl-2 levels.

JNK inhibition does not affect Bcl-2 phosphorylation: HLE-B3 cells were treated with JNK inhibitors, SP600125 (5 µM, 10 µM, or 20 µM), AS601245 (5 µM, and 10 µM,

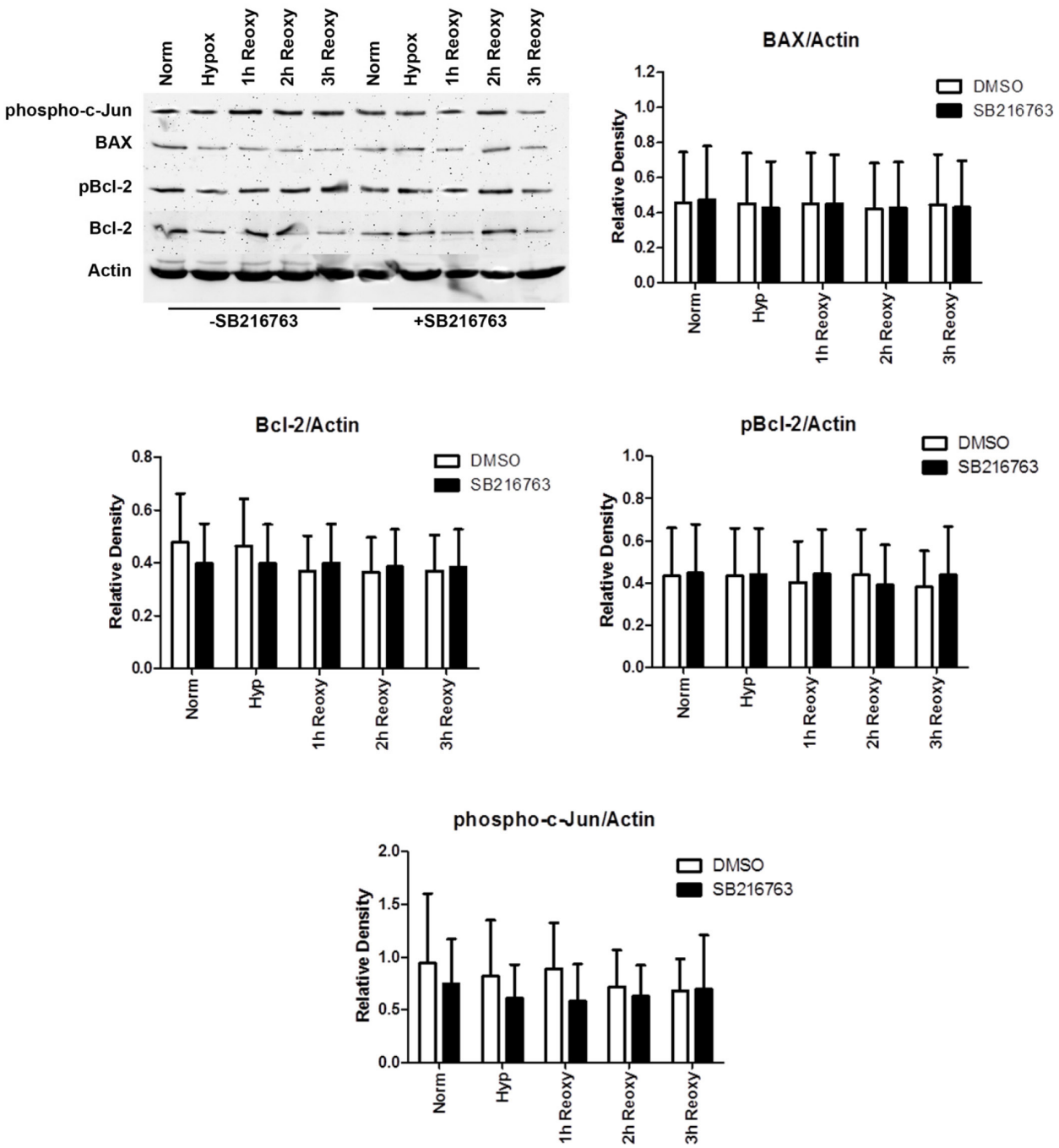

Figure 4. Western blot analysis of BAX, Bcl-2, pBcl-2, and phospho-c-Jun in HLE-B3 cells in the presence or absence of SB216763. Total cell lysates were collected from >85% confluent HLE-B3 cell cultures that were incubated for 90 min in serum-free minimal essential media (MEM), under conditions of atmospheric oxygen, containing either 12 µM SB216763) or 0.05% DMSO vehicle. Cells were then exposed to hypoxia for 3 h in the continued presence of SB216763 or DMSO vehicle. At the end of the hypoxic incubation period, the hypoxic media were removed, and fresh, oxygenated serum-free MEM with SB216763 or DMSO were added to the cultures. Cells were then placed in atmospheric oxygen for up to 3 h. Cultures were collected after (1) continuous normoxic exposure (about 21% oxygen), (2) after the 3 h hypoxic exposure (about 1% oxygen), or (3) after reintroduction of atmospheric oxygen (about 21%) for 1, 2, or 3 h subsequent to the 3 h hypoxic exposure. Total cell lysates were analyzed with immunoblots using 25 µg of protein per lane. Anti-actin was used to normalize the bands to ensure equivalent lane loading. Three experiments, using independent cell populations, were quantified using GraphPad Prism 5 and the relative densities plotted for BAX/actin, Bcl-2/actin, pBcl-2/actin, and phospho-c-Jun/Actin. No change was evident in the ratio of BAX/actin, Bcl-2/actin, pBcl-2/actin, or phospho-c-Jun/actin by treatment with SB216763. Error bars represent standard error, Student *t* test.

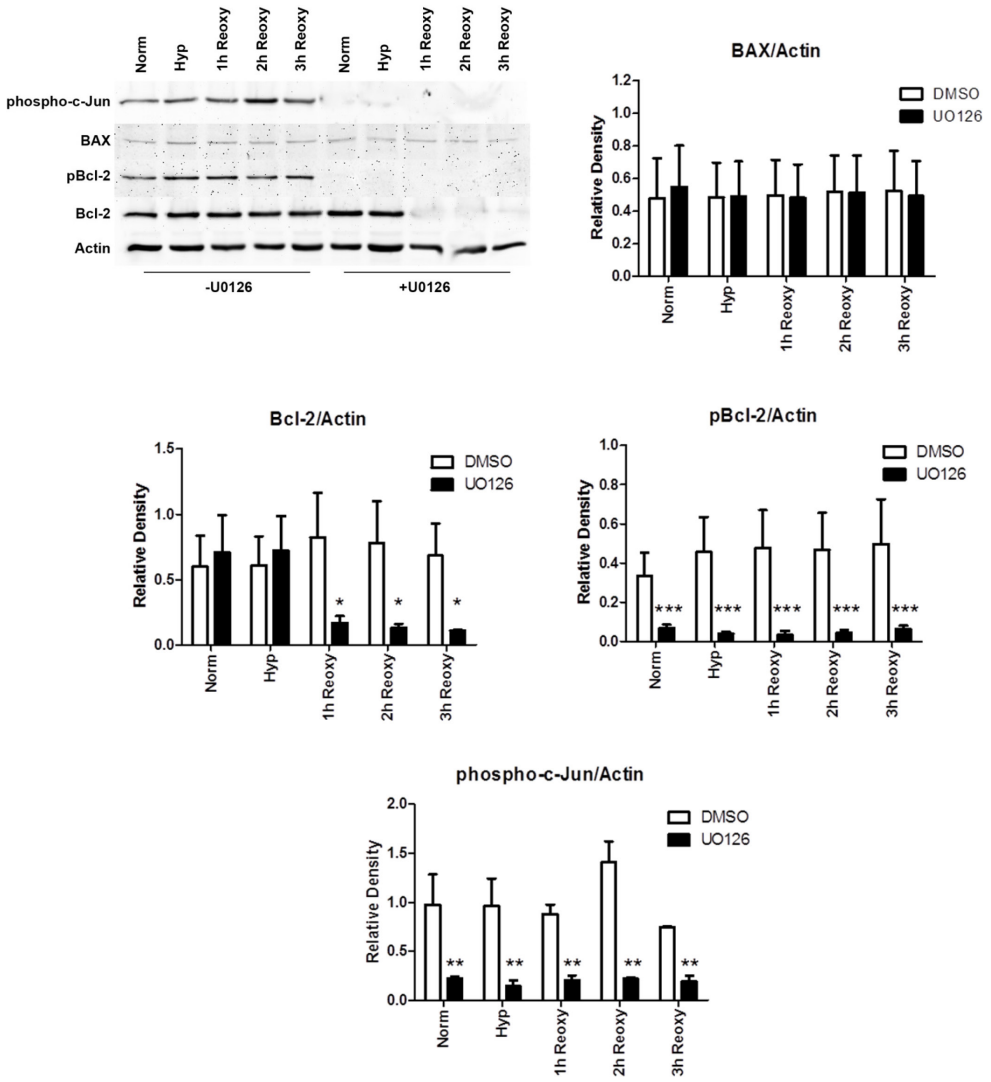

Figure 5. Western blot analysis of BAX, Bcl-2, pBcl-2, and phospho-c-Jun in HLE-B3 cells in the presence or absence of UO126. Total cell lysates were collected from >85% confluent human lens epithelial (HLE-B3) cell cultures that were incubated for 90 min in serum-free minimal essential media (MEM), under conditions of atmospheric oxygen, containing either 10 µM UO126 or 0.05% DMSO vehicle. Cells were then exposed to hypoxia for 3 h in the continuous presence of UO126 or DMSO vehicle. At the end of the hypoxic incubation period, the hypoxic media were removed, and fresh, oxygenated serum-free MEM with UO126 or DMSO were added to the cultures. Cells were then placed in atmospheric oxygen for up to 3 h in the presence or absence of SB216763. Cultures were collected after (1) continuous normoxic exposure (about 21% oxygen), (2) after the 3 h hypoxic exposure (about 1% oxygen), or (3) after reintroduction of atmospheric oxygen (about 21%) for 1, 2, or 3 h subsequent to the 3 h hypoxic exposure. Total cell lysates were analyzed with immunoblots using 25 µg of protein per lane. Anti-actin was used to normalize the bands to ensure equivalent lane loading. Three experiments, using independent cell populations, were quantified using GraphPad Prism 5. (top panel, left) The phosphorylation of c-Jun, as well as that of Bcl-2, was blocked by treatment with UO126 under all conditions as determined with western blot analysis. Interestingly, Bcl-2 levels were significantly diminished with treatment by UO126 but only upon reintroduction to atmospheric oxygen. (top panel, right) No change in relative density of the ratio of BAX/actin was evident by treatment with UO126 under any condition. Error bars represent standard error. (middle panel, left) A significant drop in Bcl-2 levels was noted but only upon reintroduction of atmospheric oxygen for the 1, 2, and 3 h incubation periods. The asterisk (*) indicates $p<0.05$, Student *t* test. (middle panel, right) A significant loss of pBcl-2 was noted under all conditions (continuous atmospheric oxygen, continuous hypoxia, and reintroduction from hypoxia to atmospheric oxygen). The asterisks (***) indicate $p<0.001$, Student *t* test. (bottom panel) Unlike with SB216763 (refer to Figure 4), treatment with UO126 resulted in a marked decrease in the phosphorylation of c-Jun, indicating that UO126 adversely affects JNK activity. The asterisks (**) indicate $p<0.01$, Student *t* test.

20 µM), or DMSO vehicle (control). Phosphorylated JNK is the active form of the enzyme, and in this form, the enzyme is capable of phosphorylating numerous downstream substrates, including c-Jun. The phosphorylation of c-Jun is thus a useful parameter for monitoring JNK activity. Treated and control cells were placed in hypoxic conditions for 3 h and then switched to atmospheric oxygen for 3 h. After the switch to atmospheric oxygen, the hypoxic media were removed from the cultures, and fresh oxygenated media containing either inhibitor or vehicle were added. Lysates of all the cells were collected after 3 h exposure in atmospheric oxygen. SP600125 and AP601245 markedly reduced phospho-c-Jun at all concentrations relative to the control cells (Figure 6). Further analysis indicated no change in the levels of BAX,

Bcl-2, or pBcl-2 for cells treated with SP600125 or AS601245 versus cells treated with DMSO vehicle (Figure 6). A slight increase in the levels of pERK were observed with either inhibitor treatment cells relative to the control cells, the meaning of which is not immediately evident to us. However, whereas UO126 negatively impacted JNK activity (Figure 5), the JNK inhibitors did not cross-inactivate ERK phosphorylation (Figure 6). We therefore concluded that inhibition of the ERK pathway, not the JNK pathway, elicited the inhibition of phosphorylation of Bcl-2 (Figure 5).

Increased mitochondrial depolarization does not necessarily affect cell viability: To determine if the inhibition of ERK or GSK-3β activity influence the onset of apoptosis, an active caspase-3 ELISA was implemented. As above, the HLE-B3 cells were treated with either 12 µM SB216763, 10 µM UO126, or 0.05% DMSO. The 100 nM staurosporine concentration was used as a positive activator of caspase-3. Cells were incubated for 90 min and then placed in hypoxia for 180 min. At the end of the hypoxic exposure, the media were removed from the treated and untreated cells, and fresh media were added. The cells were then placed in atmospheric

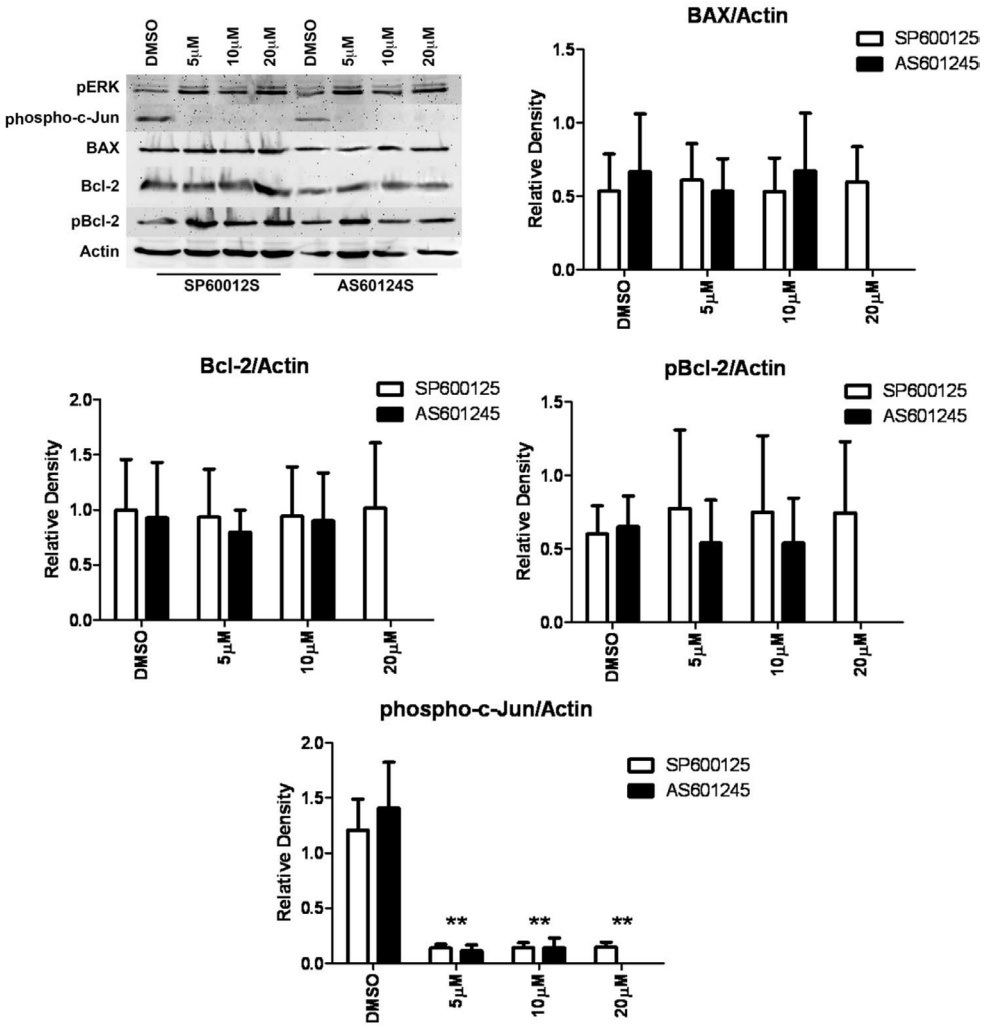

Figure 6. Western blot analysis of phospho-c-Jun in the presence of SP600125 or AS601245. HLE-B3 cell cultures were incubated for 90 min in serum-free minimal essential media (MEM), under conditions of atmospheric oxygen, containing either SP600125 (5 µM, 10 µM, and 20 µM), AS601245 (5 µM, 10 µM, and 20 µM), or DMSO (0.05%) vehicle. Cells were then exposed to hypoxia for 3 h in the continued presence of inhibitors. At the end of the hypoxic exposure, the media were removed, and fresh, oxygenated serum-free MEM with either inhibitor or DMSO were added to the cultures. Cells were subsequently placed in atmospheric oxygen for 3 h. Whole cell lysates were collected at the end of the 3 h reintroduction of atmospheric oxygen. Lysates were analyzed with western blot for phospho-c-Jun, pERK, BAX, Bcl-2, and p-BCL-2 using 25 µg of protein per lane. Anti-actin was used to normalize the bands to ensure equivalent lane loading. The inhibition of the phosphorylation of c-Jun by either JNK inhibitor indicates the inactivation of JNK activity, while no loss of BAX, Bcl-2, or pBcl-2 was noted. Under this condition, the phosphorylation of ERK was unimpeded. This experiment was performed twice with two independent cell populations with identical results. Treatment with either JNK inhibitor, SP600125 or AS601245, resulted in a marked decrease in the phosphorylation of c-Jun, indicating that both inhibitors inhibited JNK activation. The asterisks (**) indicate $p<0.01$, Student *t* test. BAX, Bcl-2, and pBcl-2 were not significantly diminished relative to the DMSO control, indicating that the ERK pathway, but not the JNK pathway, is involved in the loss of Bcl-2 and pBcl-2 (refer to Figure 5). Two experiments, using independent cell populations, were quantified using GraphPad Prism 5. Reader note: The 20 µM AS601245 was run only once as reflected in the western blot but not in the densitometry plots because we cannot generate statistics on one run.

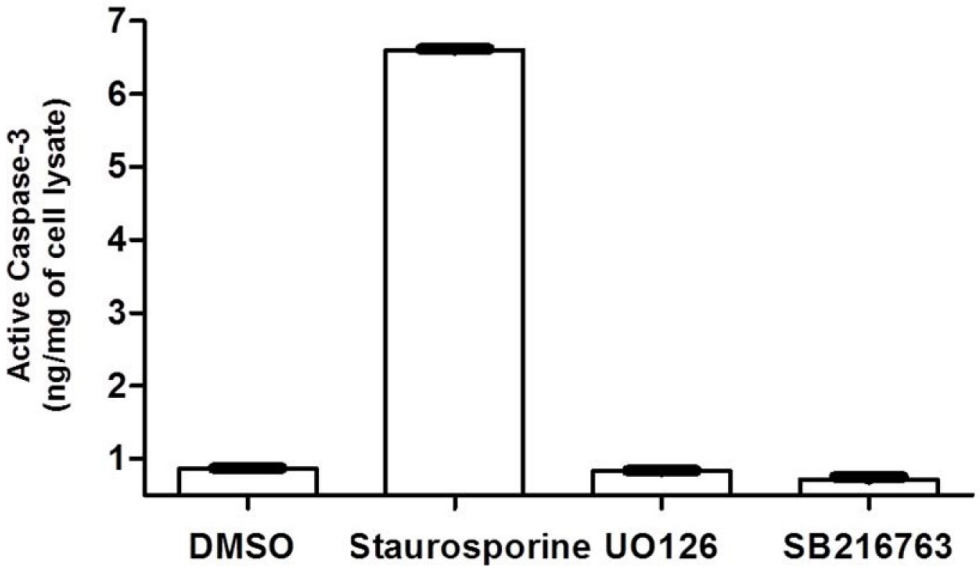

Figure 7. Active caspase-3 ELISA analysis of possible apoptosis in HLE-B3 cells treated with SB216763, UO126, staurosporine, or DMSO. The possibility of the onset of apoptosis was determined using an active capase-3 ELISA with HLE-B3 cells treated with SB216763; 12 µM), UO126; 10 µM), staurosporine (100 nM), or 0.05% DMSO vehicle. Treated and mock-treated HLE-B3 cells were incubated with serum-free minimal essential media (MEM) for 90 min in atmospheric oxygen. The cells were then switched to hypoxia for 180 min in the continued presence of each individual treatment. At the end of the hypoxic exposure, the media were removed and replaced with fresh, oxygenated media still containing SB216763, UO126, staurosporine, or DMSO vehicle. The cells were placed in atmospheric oxygen for 60 min and subsequently lysed, and the quantity of protein determined per treatment. Caspase-3 activity was determined using 10 µg of protein following the manufacturer's instructions. Data are based upon results from three independent cell populations and were analyzed using GraphPad Prism 5. The error bars represent the standard error. Only treatment with staurosporine indicated a marked increase in activation of caspase-3.

oxygen for 60 min. SB216763 and U0126 were administered throughout the duration of the experiment. At the end of this 60 min period, all samples were lysed with lysis buffer. The DMSO mock-treated cells displayed minimal capase-3 activation relative to the cells treated with staurosporine (positive control), which showed a significant increase in caspase-3 activity (Figure 7). The UO126- and SB216763-treated cells demonstrated levels of capase-3 activity similar to the DMSO mock-treated cells (Figure 7). The lack of caspase-3 activity in the UO126- and SB216763-treated cells indicate that apoptosis did not occur in the presence of either inhibitor, although the UO126 treatment elicited mitochondrial membrane permeability transition (refer to Figure 3, bottom panel).

Bovine lens epithelium portray similar responses to UO126-treatment as compared with HLE-B3 cells: To determine that our results (and consequent interpretations) had not been compromised by the viral transformation of the HLE-B3 cells, we repeated the UO126 treatment, as described above with HLE-B3 cells, with secondary cultures of normal bovine lens epithelial cells. Inhibition of p42 ERK1/2 and p44 ERK1/2 relative to the control cells was noted (Figure 8, upper panel). As with the HLE-B3 cells (Figure 3, upper panel, right), neither GSK-3β nor pGSK-3β (Figure 8, middle panel) was diminished, compared with the DMSO controls. Likewise, inhibition of ERK phosphorylation prevented the downstream phosphorylation of GS (compare Figure 3, upper panel, right and Figure 8, middle panel).

We further investigated the effect of UO126 treatment on BAX, Bcl-2, and pBcl-2 levels using secondary cultures of bovine lens epithelial cells. Lysates were evaluated with western blot analysis to determine the levels of BAX, Bcl-2, and pBcl-2. Western blot membranes from the UO126-treated cells relative to their respective controls indicated some lane loading variability, but no obvious loss, in the levels of BAX (Figure 8, bottom panel), similar to that of the HLE-B3 cells (Figure 5, upper left panel). As with the HLE-B3 cells (Figure 5, upper left panel), the UO126-treated cells displayed a significant reduction in pBcl-2 under all culture conditions: normoxic control, hypoxic exposure, and the reintroduction of oxygen (Figure 8, bottom panel). Of interest, unlike the HLE-B3 cells (Figure 5, middle panel) where a significant loss of Bcl-2 was noted (but only during the reintroduction of the oxygen phase), there was no dramatic reduction in the levels of Bcl-2 between the treated and untreated cells under any condition (Figure 8, bottom panel). Finally, as first observed with HLE-B3 cells (Figure 5, upper left panel), UO126 elicited the inhibition of phosphorylation of c-JUN, through all culture conditions (Figure 8, bottom panel).

Bovine lens epithelium depolarize in the absence of pBcl-2: Parallel studies with UO126 were conducted using JC-1 analysis. Normal bovine cell cultures were treated with 10

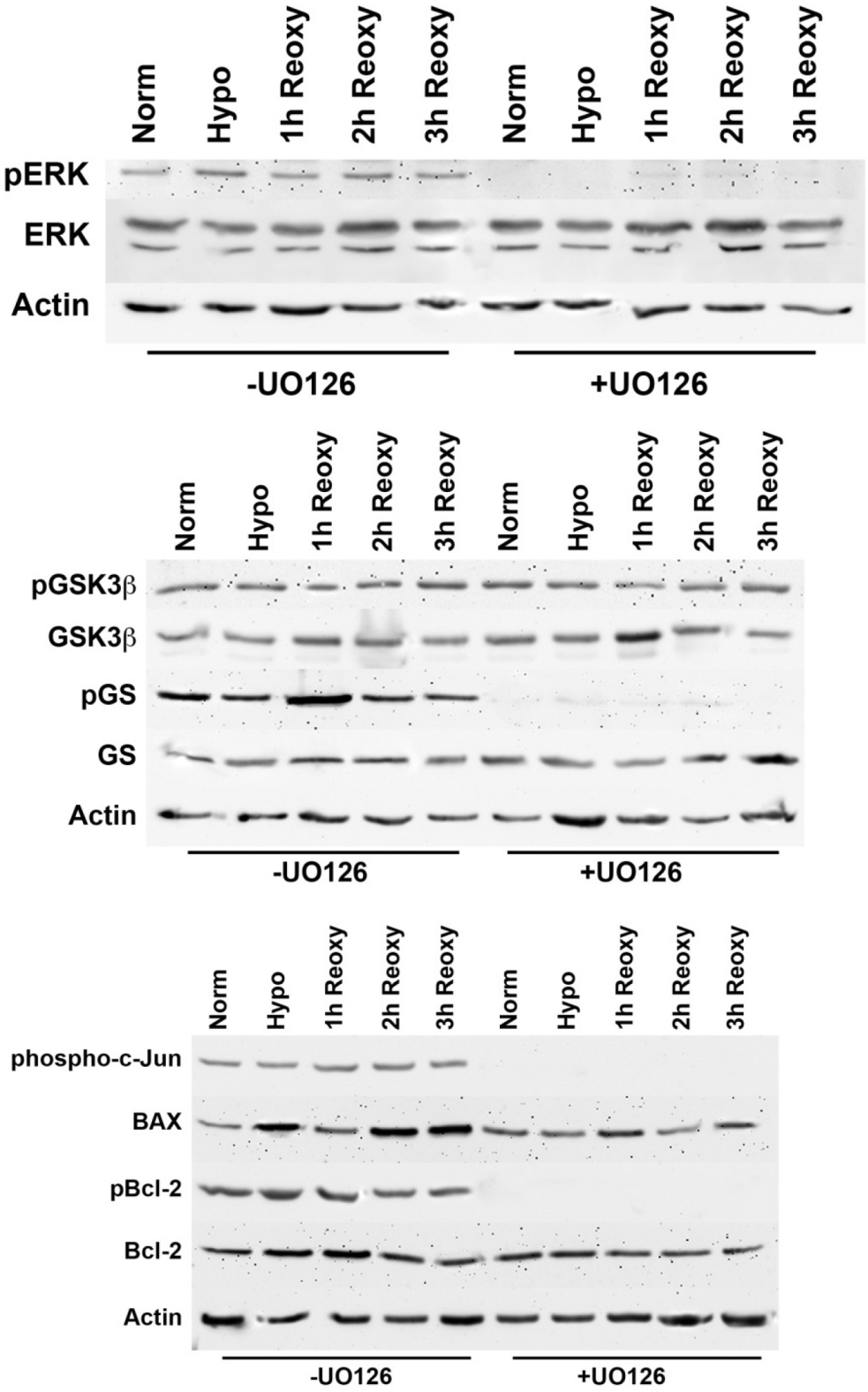

Figure 8. Western blot analysis of GSK-3β and GS phosphorylation and BAX, Bcl-2, pBcl-2, and phospho-c-Jun in secondary cultures of normal bovine cells treated with UO126 inhibitor. Bovine cell cultures were incubated for 90 min in serum-free minimal essential media (MEM), under conditions of atmospheric oxygen, containing either 10 µM UO126 or 0.05% DMSO) vehicle. Cells were then exposed to hypoxia for 3 h in the presence of either UO126 or DMSO vehicle. At the end of the hypoxic incubation period, the hypoxic media were removed, and fresh, oxygenated serum-free MEM with UO126 or DMSO were added to the cultures. Cells were then placed in atmospheric oxygen for up to 3 h. Cultures were collected after (1) continuous normoxic exposure (about 21% oxygen), (2) after the 3 h hypoxic exposure (about 1% oxygen), or (3) after reintroduction of atmospheric oxygen (about 21%) for 1, 2, or 3 h subsequent to the 3 h hypoxic exposure. Total cell lysates were analyzed with immunoblots using 25 µg of protein per lane. Anti-actin was used to normalize the bands to ensure equivalent lane loading. Prevention of phosphorylation of ERK with UO126 treatment was noted (top panel), as was the inhibition of phosphorylated glycogen synthase with western blot analysis (middle panel). The levels of GSK-3β) and pGSK-3β were consistent in the presence and absence of UO126. The phosphorylation of c-Jun, as well as that of Bcl-2, was blocked by treatment with UO126 under all conditions as determined with western blot analysis (bottom panel). Of particular note, Bcl-2 levels were unaffected by UO126 treatment compared to HLE-B3 cells (refer to Figure 5) where a significant diminution of Bcl-2 was observed but only upon reintroduction to atmospheric oxygen. No change in the relative levels of BAX was evident by treatment with UO126 under any condition. The experiment with normal, secondary cultures of bovine cells was run once, to confirm that a similar pattern of biochemical modifications by treatment with UO126 was reproducible with normal bovine cell cultures as was observed with HLE-B3, affirming that the former results were not influenced by viral transformation.

μM UO126 or DMSO and then placed under hypoxic conditions for 3 h. The cells were exposed to the JC-1 dye for 30 min in atmospheric oxygen. Following the JC-1 application, fresh media with U0126 or DMSO were added to the culture plates. The cells were subsequently observed with confocal microscopy and the green and red intensities recorded every 2.5 min for 60 min. As with the UO126-treated HLE-B3 cells (refer to Figure 3, bottom panel) the green to red ratio of the UO126-treated bovine lens cells markedly increased over the time course relative to the control cells, indicating the loss of ΔΨ (Figure 9).

DISCUSSION

To establish our reference baseline, it was first necessary to demonstrate that the experimental manipulation of switching cells from hypoxia to atmospheric oxygen or vice versa, from atmospheric oxygen to hypoxia, was not, of itself, sufficient oxidative stress to elicit mitochondrial depolarization (Figure 1). Once established that the physical manipulation of switching cell cultures from one oxygen pressure to another did not impose mitochondrial depolarization, we investigated the regulatory function of GSK-3β insofar as its ability to convey mitochondrial resistance to depolarization.

First, we sought to clarify whether blocking GSK-3β's autophosphorylation site or inactivating its catalytic active site conferred prevention of mitochondrial depolarization. To monitor the enzyme's active, catalytic site, we scrutinized the phosphorylation of a downstream substrate of GSK-3β, glycogen synthase (GS). Our data revealed that SB216763 did not block the autophosphorylation of GSK-3β relative to control cells, but successfully eliminated the phosphorylation of GS, indicating that the catalytic site of GSK-3β was inactivated (Figure 2). Stated another way, the failure to phosphorylate GS, but not the autophosphorylation site of GSK-3β, appears to be a better predictor of whether inhibiting GSK-3β's enzymatic activity positively correlates with blocking mitochondrial membrane permeability transition. In a recent report using the specific GSK-3β inhibitor, SB216763, we demonstrated that "inhibition of GSK-3β activity by SB216763 blocked mitochondrial membrane permeability transition relative to the slow but consistent depolarization observed with the control cells." We concluded that inhibiting GSK-3β activity with the GSK-3β inhibitor SB216763 provides positive protection against mitochondrial depolarization [18].

The role of GSK-3β and how it may be influenced by upstream signaling mechanisms has been the focus of numerous studies. "There is evidence in different cell types [19] that anti-apoptotic responses can be mediated by phosphatidylinositol 3-kinase (PI3K) and the Akt/PKB serine-threonine protein kinase, p42/p44 mitogen-activated protein kinases or extracellular response kinases (ERKs), Raf, and cyclic AMP-dependent protein kinase (PKA)." To further delve into this issue, using the lens cell model, we compared and contrasted the pGSK-3β /GSK-3β, as well as the pGS /GS western blot profiles of cells treated with an inhibitor of ERK against the known catalytic site inhibitor of GSK-3β, SB216763 (refer to above). We followed up with a JC-1 evaluation to monitor whether ERK inhibitor treatment prompted mitochondrial depolarization or whether, like SB216763, inhibiting ERK phosphorylation imposed resistance to mitochondrial depolarization [18].

Similar to the treatment with SB216763 (Figure 2), treatment with UO126 had no effect on autophosphorylation of GSK-3β relative to the control cells, but successfully eliminated the phosphorylation of GS (Figure 3, upper panel, right). However, whereas treatment with SB216763 resulted in suppression of mitochondrial depolarization [18], unexpectedly, the UO126-treated cells displayed profound depolarization (Figure 3, bottom panel). We therefore sought to explain the apparent discrepancy between the similarity of the SB216763 and UO126 profiles of pGSK-3β/GSK-3β and pGS/GS and the observation that the former [18] but not the latter (Figure 3) conferred resistance to mitochondrial depolarization.

Western blot analysis of HLE-B3 cells treated with SB216763 or UO126 showed that the BAX levels were unchanged relative to the untreated, control cells (compare Figure 4 versus Figure 5). Moreover, the BAX content of the UO126-treated normal bovine lens epithelial cells was similar relative to the control cells (Figure 8, bottom panel). These data support the notion that BAX does not play a direct role in lens epithelial cell resistance to mitochondrial depolarization. We therefore directed our attention to answering the question, "Is it the continuous expression of Bcl-2 or the phosphorylation of Bcl-2 that confers resistance to mitochondrial depolarization?" The UO126-treated virally transformed HLE-B3 cells, and the normal bovine lens epithelial cells demonstrated a propensity to depolarize (compare Figure 3, bottom panel and Figure 9). We took advantage of our observation that UO126 treatment with HLE-B3 cells instigated a loss of Bcl-2 (but only under the condition of reintroduction of oxygen (refer to Figure 5) whereas UO126-treatment with normal bovine lens epithelial cells did not diminish the levels of Bcl-2 (Figure 8, bottom panel), this although with both types of cells, a profound loss of pBcl-2 was apparent under all conditions (compare Figure 5, top panel, left with Figure 8, bottom panel). Therefore, since the bovine cells depolarized

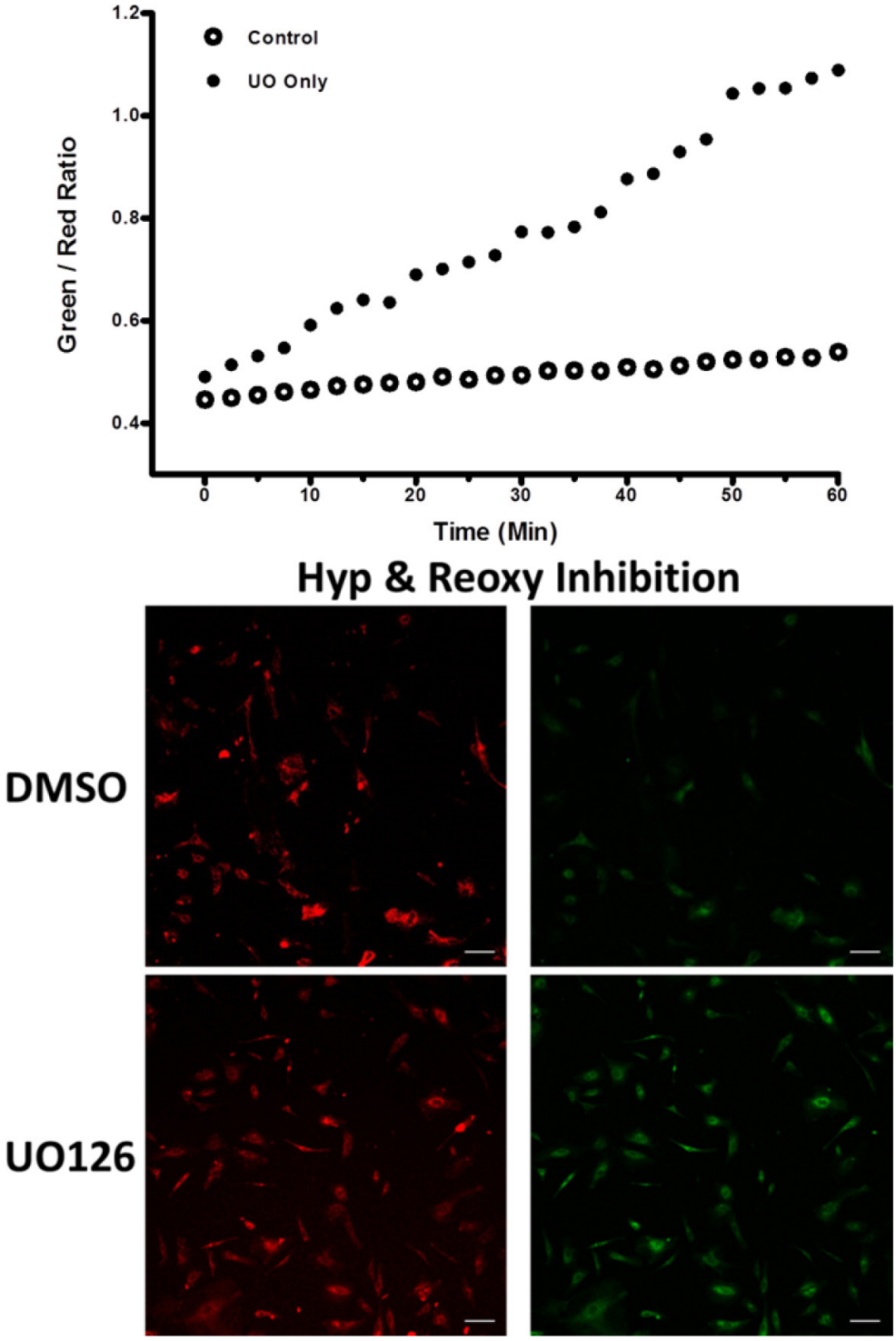

Figure 9. JC-1 analysis of bovine lens epithelial cells treated with UO126 inhibitor. Secondary cultures of bovine lens epithelial cells were incubated for 90 min with serum-free minimal essential media (MEM), under atmospheric condition, containing 10 µM UO126 or 0.05% DMSO vehicle. Cells were switched to hypoxia for 3h in the continued presence or absence of UO126. At the end of the hypoxic exposure, the cell media were removed, and fresh, oxygenated serum-free MEM containing 5 µg/ml JC-1 and either UO126 or DMSO added for 30 min in atmospheric oxygen. At the end of the 30 min incubation period, the media were again switched to fresh serum-free MEM containing UO126 or DMSO in the absence of the JC-1 dye. A random field of cells was chosen, and that field of cells was imaged every 150 s for 60 min. Serial confocal imaging of mitochondrial depolarization of the secondary cultures of normal bovine lens epithelial cells in the presence of UO126 demonstrated significant depolarization compared to control cells (top panel). Images of the red and green intensity (bottom panel) for the UO126- and DMSO-treated cells at t=60 min (bar=20 µm) are shown (bottom panel). Note the marked intensity of the green channel with the UO126-treated cells relative to DMSO mock treatment at the completion of the 60 min analysis, which indicates a propensity toward a significant degree of mitochondrial depolarization.

without the loss of Bcl-2, we conclude that pBcl-2 confers anti-depolarization resistance in lens epithelial cells.

Lei et al. 2002 [20-24] stated, “this phosphorylation has been reported to inhibit the pro-survival function of Bcl. This conclusion, however, is controversial as other studies have indicated that phosphorylation may enhance the anti-apoptotic actions of Bcl-2” [25-27]. Data from our study lend support to the latter statement in that the depolarization observed with UO126 treatment is caused by a lack of pBcl-2 (compare Figure 3 and Figure 5 with Figure 8 and Figure

9). The lack of pBcl-2 likely results in a loss of Bcl-2's anti-apoptotic function as reported by others. Cellular apoptosis is regulated, in part, by maintaining a balance between the levels of the prosurvival protein, Bcl-2, and the proapoptotic protein, BAX. BAX is a proapoptotic member of the Bcl-2 family. Activation of BAX causes its translocation to the mitochondrial outer membrane and induces mitochondrial depolarization. However, before BAX can initiate this process, the protein must first translocate from the cytoplasm to the mitochondria. Bcl-2 influences apoptosis by regulating the translocation of BAX to the mitochondria [28,29]. Any decrease in the levels of Bcl-2 (or in our case, pBcl-2) is likely to permit the translocation of BAX from the cytosol to the mitochondria and induce mitochondrial depolarization. Disruption of the integrity of the outer mitochondrial membrane would then be the cause of the initiation of the loss of $\Delta\Psi$, often cited as an early predictor of the onset of apoptosis.

Previous studies in our laboratory have shown that UO126 inhibits not only ERK phosphorylation but also JNK activity (unpublished data). Studies have shown that pJNK mediates the phosphorylation of the antiapoptotic protein Bcl-2 [20-25]. Thus, as this relates to the studies described here, one possible explanation for the loss of mitochondrial membrane potential could have been attributed to the loss of JNK activity. To determine whether this was the case, we analyzed JNK activity with UO126 treatment. A common measure of JNK activity is to monitor the phosphorylation of one of its downstream substrates, c-Jun, where inhibition of the phosphorylation of c-Jun indicates inactivation of JNK. The level of phospho-c-Jun was similar with SB216763 treatment relative to control cells (Figure 4). UO126 inhibited c-Jun phosphorylation (Figure 5). Moreover, the resulting inhibition of c-Jun phosphorylation with treatment by UO126 was accompanied by an apparent loss of pBcl-2, thus suggesting a potential connection between the JNK pathway and mitoprotection (Figure 5). UO126 treatment, since it inhibited JNK activity, complicated our ability to definitively interpret the data, in that our results would not permit us to immediately distinguish whether the inhibition of phosphorylation of ERK or JNK influenced the downstream reduction in pBcl-2 levels.

It therefore became necessary to determine which of the two pathways, ERK or JNK, was influencing the phosphorylation of Bcl-2. HLE-B3 cells were treated with two specific inhibitors of JNK activation. Analysis of the levels of phospho-c-Jun revealed that SP600125 and AS601245 effectively reduced the levels of phospho-c-Jun relative to that of the controls without affecting the pBcl-2 levels (Figure 6). Collectively, the data reported in Figure 5 and Figure 6 allowed us to assert that inactivating JNK does not influence Bcl-2 phosphorylation. Instead, inhibiting ERK causes the loss of Bcl-2 phosphorylation. We therefore conclude that inhibiting ERK phosphorylation overrides the mitoprotection otherwise afforded by SB216763 presumably because of the loss of pBcl-2 (Figure 5 and Figure 8).

Mitochondrial depolarization is often cited as an early indicator of the onset of apoptosis. However, our studies establish that despite the mitochondrial depolarization initiated by UO126 treatment for HLE-B3 cells (Figure 3, bottom panel) in conjunction with the loss of pBcl-2 (Figure 5), the degree of the mitochondrial membrane permeability transition was at an insufficient level to induce apoptosis in human lens epithelial cells, as indicated by the lack of active caspase-3 (Figure 7). Our result is not all that unexpected because it has previously been shown that there is considerable intracellular heterogeneity in mitochondrial membrane potential of mitochondria [30]. In effect, the degree of mitochondrial depolarization as indicated by the JC-1 dye represents the collective states of depolarization from a heterogeneous population of mitochondria. We conclude that one must exercise caution when equating mitochondrial depolarization with the onset of apoptosis. Cellular apoptosis/necrosis should be determined only after examination with annexin V/propidium iodide, DNA fragmentation, or caspase-3 or -9 cleavage, or some combination thereof.

In conclusion, the studies presented here further support our previous assertion [18] that GSK-3β is a critical upstream regulator of mitochondrial membrane permeability transition for human lens epithelial cells cultured in atmospheric oxygen. In this study, we have established a direct relationship between the active catalytic site of GSK-3β and the normal functioning of the mitochondrial permeability transition pore to open and close. However, inhibiting ERK phosphorylation indirectly overrides the otherwise protective influence of GSK-3β to resist mitochondrial membrane permeability transition through a concomitant loss of pBcl-2 levels leading to mitochondrial depolarization. Restated, the fact that SB216763 and UO126 prevent the phosphorylation of GS suggests that GS phosphorylation, itself, may be regulated by one of the many signaling pathways activated by ERK independent of GSK-3β. At the same time, the ERK pathway also likely independently influences Bcl-2 phosphorylation. The mechanism by which UO126 administration leads to preventing phosphorylation of Bcl-2 is currently not understood and warrants further investigation.

Recent studies in our laboratory have shown that UO126 treatment elicits a significant decrease in the expression of

vascular endothelial growth factor (VEGF) but only upon reintroduction from hypoxia to atmospheric oxygen (unpublished observation). However, UO126 does not have an effect on VEGF expression in hypoxia-maintained cells [31]. VEGF acts as a prosurvival factor in hypoxic lens epithelial cells by maintaining consistent expression of the prosurvival protein Bcl-2, which likely prevents the translocation of cytosolic BAX to the outer mitochondrial membrane, thus preventing the initiation of mitochondrial depolarization [31]. Our laboratory is interested in regulating VEGF as a cell survival protein. Current studies in the laboratory are directed toward elucidating the potential role of GSK-3β in managing the sustained expression of VEGF and how VEGF expression regulates the levels of Bcl-2 and its phosphorylated counterpart as it influences downstream impact on lenticular mitoprotection in atmospheric oxygen (manuscript in preparation).

ACKNOWLEDGMENTS

The authors express their gratitude to Lawrence Oakford for the preparation of all figures and images in this manuscript and to I-Fen Chang for technical support in obtaining the JC-1 image analysis data.

REFERENCES

1. Flynn JM, Lannigan DA, Clark DE, Garner MH, Cammarata PR. RNA suppression of ERK2 leads to collapse of mitochondrial membrane potential with acute oxidative stress in human lens epithelial cells. Am J Physiol Endocrinol Metab 2008; 294:E589-99. [PMID: 18171912].
2. Farber JL, Kyle ME, Coleman JB. Mechanisms of cell injury by activated oxygen species. Lab Invest 1990; 62:670-9. [PMID: 2162996].
3. Baines CP. The molecular composition of the mitochondrial permeability transition pore. J Mol Cell Cardiol 2009; 46:850-7. [PMID: 19233198].
4. Crow MT, Mani K, Nam YJ, Kitsis RN. The mitochondrial death pathway and cardiac myocyte apoptosis. Circ Res 2004; 95:957-70. [PMID: 15539639].
5. Halestrap A. Biochemistry: a pore way to die. Nature 2005; 434:578-9. [PMID: 15800609].
6. Juhaszova M, Zorov DB, Kim SH, Pepe S, Fu Q, Fishbein KW, Ziman BD, Wang S, Ytrehus K, Antos CL, Olson EN, Sollott SJ. Glycogen synthase kinase-3beta mediates convergence of protection signaling to inhibit the mitochondrial permeability transition pore. J Clin Invest 2004; 113:1535-49. [PMID: 15173880].
7. Di Lisa F, Canton M, Menabo R, Kaludercic N, Bernardi P. Mitochondria and cardioprotection. Heart Fail Rev 2007; 12:249-60. [PMID: 17516167].
8. Murphy E, Steenbergen C. Mechanisms underlying acute protection from cardiac ischemia-reperfusion injury. Physiol Rev 2008; 88:581-609. [PMID: 18391174].
9. Juhaszova M, Zorov DB, Yaniv Y, Nuss HB, Wang S, Sollott SJ. Role of glycogen synthase kinase-3beta in cardioprotection. Circ Res 2009; 104:1240-52. [PMID: 19498210].
10. Gomez L, Paillard M, Thibault H, Derumeaux G, Ovize M. Inhibition of GSK3beta by postconditioning is required to prevent opening of the mitochondrial permeability transition pore during reperfusion. Circulation 2008; 117:2761-8. [PMID: 18490522].
11. Förster K, Richter H, Alexeyev MF, Rosskopf D, Felix SB, Krieg T. Inhibition of glycogen synthase kinase 3beta prevents peroxide-induced collapse of mitochondrial membrane potential in rat ventricular myocytes. Clin Exp Pharmacol Physiol 2010; 37:684-8. [PMID: 20337662].
12. Rasola A, Sciacovelli M, Chiara F, Pantic B, Brusilow WS, Bernardi P. Activation of mitochondrial ERK protects cancer cells from death through inhibition of the permeability transition. Proc Natl Acad Sci USA 2010; 107:726-31. [PMID: 20080742].
13. Andley UP, Rhim JS, Chylack LT Jr, Fleming TP. Propagation and immortalization of human lens epithelial cells in culture. Invest Ophthalmol Vis Sci 1994; 35:3094-102. [PMID: 8206728].
14. Henrich LM, Smith JA, Kitt D, Errington TM, Nguyen B, Traish AM, Lannigan DA. Extracellular signal-regulated kinase 7, a regulator of hormone-dependent estrogen receptor destruction. Mol Cell Biol 2003; 23:5979-88. [PMID: 12917323].
15. Salvioli S, Ardizzoni A, Franceschi C, Cossarizza A. JC-1, but not DiOC6(3) or rhodamine 123, is a reliable fluorescent probe to assess delta psi changes in intact cells: implications for studies on mitochondrial functionality during apoptosis. FEBS Lett 1997; 411:77-82. [PMID: 9247146].
16. Cohen P, Frame S. The renaissance of GSK3. Nat Rev Mol Cell Biol 2001; 2:769-76. [PMID: 11584304].
17. Cole A, Frame S, Cohen P. Further evidence that the tyrosine phosphorylation of glycogen synthase kinase-3 (GSK3) in mammalian cells is an autophosphorylation event. Biochem J 2004; 377:249-55. [PMID: 14570592].
18. Brooks MM, Neelam S, Fudala R, Gryczynski I, Cammarata PR. Lenticular mitoprotection. Part A: Monitoring mitochondrial depolarization with JC-1 and artifactual fluorescence by the glycogen synthase kinase-3beta inhibitor, SB216763. Mol Vis 2013; 19:1406-12. [PMID: 23825920].
19. Jarpe MB, Widmann C, Knall C, Schlesinger TK, Gibson S, Yujiri T, Fanger GR, Gelfand EW, Johnson GL. Anti-apoptotic versus pro-apoptotic signal transduction: checkpoints and stop signs along the road to death. Oncogene 1998; 17:1475-82. [PMID: 9779994].
20. Lei K, Nimnual A, Zong WX, Kennedy NJ, Flavell RA, Thompson CB, Bar-Sagi D, Davis RJ. The Bax subfamily of Bcl2-related proteins is essential for apoptotic signal

transduction by c-Jun NH(2)-terminal kinase. Mol Cell Biol 2002; 22:4929-42. [PMID: 12052897].

21. Fan M, Goodwin M, Vu T, Brantley-Finley C, Gaarde WA, Chambers TC. Vinblastine-induced phosphorylation of Bcl-2 and Bcl-XL is mediated by JNK and occurs in parallel with inactivation of the Raf-1/MEK/ERK cascade. J Biol Chem 2000; 275:29980-5. [PMID: 10913135].

22. Kharbanda S, Saxena S, Yoshida K, Pandey P, Kaneki M, Wang Q, Cheng K, Chen YN, Campbell A, Sudha T, Yuan ZM, Narula J, Weichselbaum R, Nalin C, Kufe D. Translocation of SAPK/JNK to mitochondria and interaction with Bcl-x(L) in response to DNA damage. J Biol Chem 2000; 275:322-7. [PMID: 10617621].

23. Maundrell K, Antonsson B, Magnenat E, Camps M, Muda M, Chabert C, Gillieron C, Boschert U, Vial-Knecht E, Martinou JC, Arkinstall S. Bcl-2 undergoes phosphorylation by c-Jun N-terminal kinase/stress-activated protein kinases in the presence of the constitutively active GTP-binding protein Rac1. J Biol Chem 1997; 272:25238-42. [PMID: 9312139].

24. Yamamoto K, Ichijo H, Korsmeyer SJ. BCL-2 is phosphorylated and inactivated by an ASK1/Jun N-terminal protein kinase pathway normally activated at G(2)/M. Mol Cell Biol 1999; 19:8469-78. [PMID: 10567572].

25. Deng X, Xiao L, Lang W, Gao F, Ruvolo P, May WS Jr. Novel role for JNK as a stress-activated Bcl2 kinase. J Biol Chem 2001; 276:23681-8. [PMID: 11323415].

26. Ito T, Deng X, Carr B, May WS. Bcl-2 phosphorylation required for anti-apoptosis function. J Biol Chem 1997; 272:11671-3. [PMID: 9115213].

27. Ruvolo PP, Deng X, May WS. Phosphorylation of Bcl2 and regulation of apoptosis. Leukemia 2001; 15:515-22. [PMID: 11368354].

28. Murphy KM, Ranganathan V, Farnsworth ML, Kavallaris M, Lock RB. Bcl-2 inhibits Bax translocation from cytosol to mitochondria during drug-induced apoptosis of human tumor cells. Cell Death Differ 2000; 7:102-11. [PMID: 10713725].

29. Nomura M, Shimizu S, Ito T, Narita M, Matsuda H, Tsujimoto Y. Apoptotic cytosol facilitates Bax translocation to mitochondria that involves cytosolic factor regulated by Bcl-2. Cancer Res 1999; 59:5542-8. [PMID: 10554032].

30. Smiley ST, Reers M, Mottola-Hartshorn C, Lin M, Chen A, Smith TW, Steele GD Jr, Chen LB. Intracellular heterogeneity in mitochondrial membrane potentials revealed by a J-aggregate-forming lipophilic cation JC-1. Proc Natl Acad Sci USA 1991; 88:3671-5. [PMID: 2023917].

31. Neelam S, Brooks MM, Cammarata PR. Lenticular cytoprotection. Part 1: The role of hypoxia inducible factors-1alpha and −2alpha and vascular endothelial growth factor in lens epithelial cell survival in hypoxia. Mol Vis 2013; 19:1-15. [PMID: 23335846].

Articles are provided courtesy of Emory University and the Zhongshan Ophthalmic Center, Sun Yat-sen University, P.R. China. The print version of this article was created on 29 November 2013. This reflects all typographical corrections and errata to the article through that date. Details of any changes may be found in the online version of the article.